Springer

Journal of Mechanical Science and Technology 22 (2008) 1945~1951

Journal of Mechanical Science and Technology

www.springerlink.com/content/1738-494x
DOI 10.1007/s12206-008-0736-7

Effect of hole shape on the heat transfer in a rectangular duct with perforated blockage walls †

Somin Shin and Jae Su Kwak*

School of Aerospace and Mechanical Engineering, Korea Aerospace University
200-1 Hwajeon-Dong, Deogyang-Gu, Goyang-City, Gyeonggi-Do, 412-791, Korea

(Manuscript Received April 16, 2008; Revised July 1, 2008; Accepted July 23, 2008)

Abstract

Heat transfer coefficients were measured by the improved hue detection based liquid crystal technique in a turbine blade internal cooling passage model with blockage walls. In the experiments, blockages with 9 holes of circular, wide, narrow shapes were used and for the circular shape, the number of hole of 7, 9, and 11 were tested. For all cases, the perforated area was kept same. Results showed that the staggered impingement jets increased heat transfer coefficient, however, pressure drop also increased greatly. Generally, Nusselt number ratio and the thermal performance factor decreased as Reynolds number increased. For all Reynolds numbers tested, the blockage wall with wide holes gave more uniform heat transfer coefficient and higher thermal performance factor. As the number of hole increased from 7 to 11, the distribution of heat transfer coefficient became uniform and the thermal performance factor increased.

Keywords: Turbine blade cooling; Impingement cooling; Staggered jets; Thermal performance factor

1. Introduction

Gas turbine inlet temperature has been increased in order to increase the efficiency and power output of the gas turbine engine. As a result, heat load to gas turbine components also increased and various cooling technique has been applied in order to ensure performance and life of the components. For the gas turbine blades, rib turbulated cooling, pin-fin cooling, and impingement cooling are applied in blade's internal coolant passage in order to remove heat from the blade inside. Fig. 1 presents the commonly used turbine blade internal cooling techniques. On the blade external surface, film-cooling method is employed in order to protect the blade surface from the hot combustion gas. Recently, new concept of trailing edge internal cooling technique which utilizes repeated impingement jets has been proposed and studied. Perforated walls make jets and impinge on the downstream walls. It is expected that the impingement and mixing of coolant would increase internal heat transfer coefficient. Ekkad et al. [1] and Pamula et al. [2] used liquid crystals and smoke for heat transfer study and flow visualization in a two-pass channel separated by a dividing wall with an array of holes. They showed that jet by the holes impinged on the next wall and swirling cross flows were induced in the second passage. Moon and Lau [3] measured pressure drop and heat transfer coefficient by liquid crystal technique on the rectangular duct with perforated walls. They showed that the number of walls and configuration of holes did not affect the heat transfer level. Their results also showed that the smaller holes could increase heat transfer coefficient but pressure drop also greatly increased. Lau et al. [4] examined the heat transfer and pressure drop on a rectangular duct with perforated walls equipped with staggered holes. They showed that walls with circular holes and

† This paper was presented at the 9th Asian International Conference on Fluid Machinery (AICFM9), Jeju, Korea, October 16-19, 2007.

*Corresponding author. Tel.: +82 2 300 0103, Fax.: +82 2 3158 3189
E-mail address: jskwak@kau.ac.kr

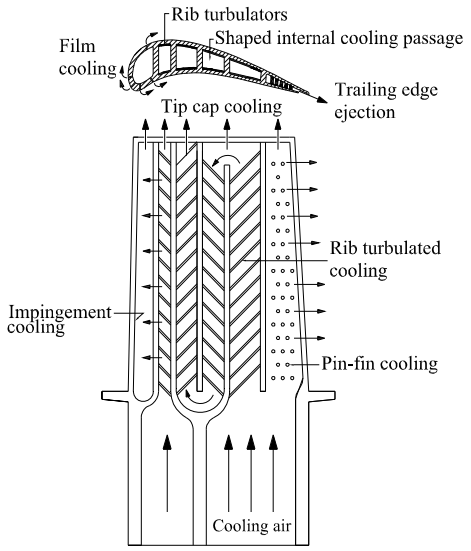

Fig. 1. Commonly used gas turbine blade internal cooling technique.

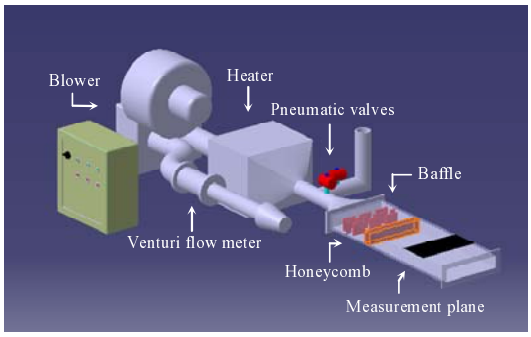

Fig. 2. Schematic of test facility (not to scale).

square holes increased heat transfer but the increase in pressure drop was much severe. They concluded that the shape and size of holes should be optimized in order to get better thermal performance ratio.

In this study, five shapes of hole were tested in order to examine the effect of hole shape on the heat transfer and pressure drop in a rectangular duct with repeated impingement jet holes. The shapes of the tested hole were narrow, wide, and circular. For the circular hole, the numbers of fabricated hole on each blockage wall were 7, 9, and 11. For all cases, the flow area of each blockage wall was kept same. Reynolds number based on the duct hydraulic diameter was changed from about 20000 to 40000. Improved hue detection based transient liquid crystal technique [5] was used for the heat transfer measurement.

2. Experiment set up

Test facility consists of a Venturi flow meter with a differential pressure transmitter (Rosemount, 250in H_2O), a blower (p_{max}=4800 mm H_2O, Q_{max}=9.8 m^3/min), a electrical heater (12 kW), and two pneumatic valves. Fig. 2 shows the schematic of test facility. The flow rate is measured by a Venturi flow meter and calculated by Eq. (1) [6].

$$Q = \frac{C_d}{\sqrt{1-\beta^4}} \varepsilon \frac{1}{4} \pi d^4 \sqrt{\frac{2\Delta p}{\rho}} \tag{1}$$

Heated air is bypassed until the air temperature reaches preset value. After the air temperature becomes predetermined value, air is diverted to the test section by pneumatic valves. In order to ensure the uniform inlet flow, baffles and honeycomb were installed between duct inlet and measurement plane as shown in Fig. 2.

Fig. 3(a) presents the configuration of test section and shapes of hole used in the test. Test section was built of 10 mm transparent polycarbonate plate. Thermocouples or pressure taps were installed upstream, between, and downstream from the blockage walls. For the heat transfer and pressure measurement, two different upper plates with thermocouples or pressure taps were used. Liquid crystals (35C1W, Hallcrest) with bandwidth of 1℃ were sprayed on the heat transfer measurement planes and digital CCD camera and incandescent lamps were installed above the test section. During the heat transfer measurement, the color change of liquid crystals was stored in a computer through IEEE1394 cable in a rate of 30 frames per second, DV format AVI file. From the every pixel of each frame of the AVI file, RGB(red, green, and blue) values are calculated and converted to 8 bit HSI(hue, saturation, and intensity) by Matlab based image processing program developed by authors. For the heat transfer coefficient calculation, an improved transient liquid crystal technique was used. By using this technique, the unstable hue behavior in low intensity condition and noise effect on hue can be reduced and more accurate hue change time can be evaluated. Detailed image processing procedure and the improved transient liquid crystal technique were described by Shin and Kwak [5]. During the transient tests, the change of mainstream temperature was measured by 4 T-type thermocouples and recorded by data acquisition device (Aglient, 34970A) connected

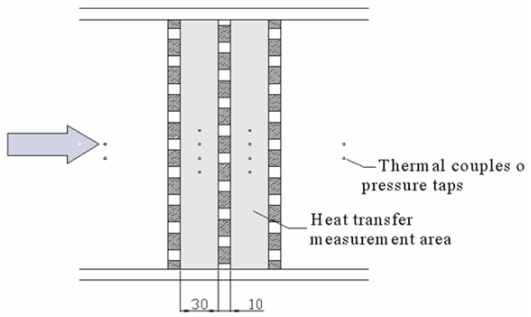

(a) Layout of blockages

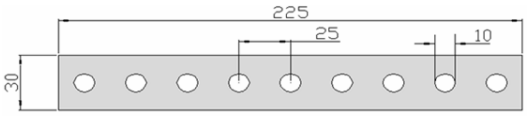

(b) Circular holes

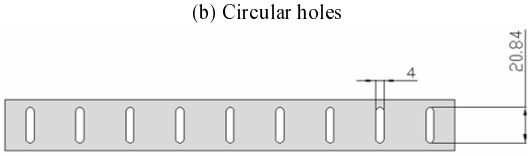

(c) Narrow holes

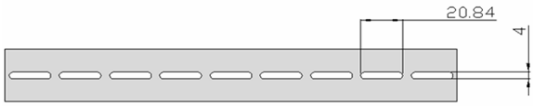

(d) Wide holes

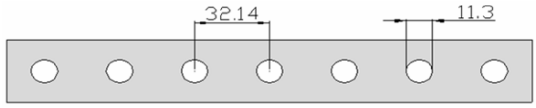

(e) Circular 7 holes

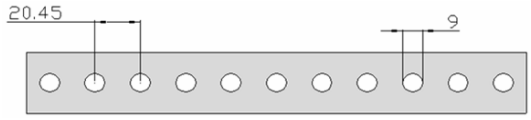

(d) Circular 11 holes

Fig. 3. Configuration of test section.

to the computer.

Figs. 3(b), (c), (d), (e), and (f) present blockage walls with circular 9 , narrow, wide, circular 7, and circular 11 holes, respectively. For all cases, overall flow area was same. The thickness of the blockage wall was 10 mm and the distance between blockage walls were 30 mm. Each row or hole was located so that upstream jets impinge between the downstream holes.

3. Heat transfer measurement theory

In the transient liquid crystal technique, the test surface is assumed as a semi-infinite solid wall with convective boundary condition. If the sudden change in mainstream temperature or velocity is applied to the test section, the surface temperature changes with time and the heat transfer coefficient can be calculated by utilizing time between the initial temperature to the preset surface temperature. Basic equation, initial, and boundary condition are as followings;

$$k_w \frac{\partial^2 T}{\partial x^2} = \rho_w c_p \frac{\partial T}{\partial t} \tag{2}$$

$$at \;\; t = 0, T = T_i \tag{3}$$

$$at \;\; x = 0, -k_w \frac{\partial T}{\partial t} = h(T_w - T_m) \tag{4}$$

$$as \;\; x \to \infty, T = T_i \tag{5}$$

If mainstream temperature varies with time, which commonly occurs in internal heat transfer tests, these variations are assumed as step changes and solution of above equation at surface (x=0) can be expressed as Eq. (6).

$$T_w - T_i = \left(T_{m,0} - T_i\right) \times F\left(\frac{h\sqrt{\alpha t}}{k_w}\right) + \sum_{j=1}^{n}\left[F\left(\frac{h\sqrt{\alpha\left(t-\tau_j\right)}}{k_w}\right)\Delta T_{m,j}\right] \tag{6}$$

where, $F(x) = 1 - \exp\left(x^2\right) erfc(x)$,
$\Delta T_{m,j}$ = temperature step change of main flow

In this study, because $T_{m,0}$ and T_i are equal, thus the first term of Eq. (6) become zero. Thus, once the time (t) from initial temperature (T_i) to pre-defined temperature (T_w) is given, heat transfer coefficient can be calculated by Eq. (6).

Surface temperature (T_w) is corresponding to the hue value of 50 and obtained from pre-operated hue-temperature calibration. For the hue-temperature calibration, copper plate was attached on the hot side of thermoelectric element using high conductive glue. T-type thermocouples were instrumented on the copper plate and 1℃ bandwidth liquid crystals(35C1W, Hallcrest) was sprayed on the copper plate after black paint was applied on. By changing the temperature of the copper plate by 0.1℃ step, the color of liquid

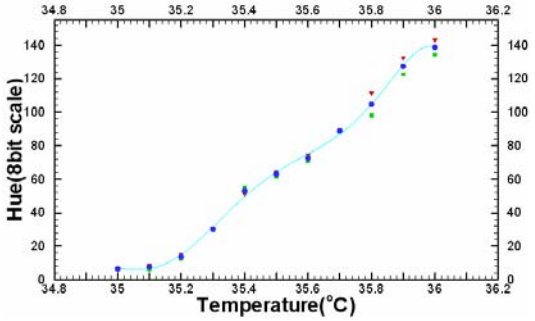

Fig. 4. Relation between temperature and hue.

crystals coated surface was recorded and hue value was calculated. Fig. 4 shows the relation between the calculated hue and the temperature obtained by thermocouple couples. Mainstream temperature (T_m) is local averaged temperature measured by four T-type thermocouples on each measurement plane as shown in Fig. 3(a).

Augmentation of heat transfer by impingement or turbulator accompanies pressure drop. Thus, the heat transfer augmentation should be compared with the pressure drop in order to evaluate the thermal performance of heat transfer enhancing method. In this study, thermal performance factor defined by Eq. (7) was used.

$$TP = \frac{\overline{Nu_{D_h}} / Nu_{D_h,0}}{\left(f / f_0\right)^{1/3}} \tag{7}$$

In Eq. (7), f_0 is the friction factor for fully developed turbulent flow in the smooth tube, f is the Darcy friction factor calculated from pressure measurement, $Nu_{D_h,0}$ is Nusselt number for fully developed turbulent flow in smooth tubes with the same hydraulic diameter, and Nu_{D_h} is measured Nusselt number. f is defined as Eq. (8).

$$f = \frac{-(\Delta p / \Delta x)\, D_h}{\rho_m\, \overline{u}^2 / 2} \tag{8}$$

In Eq. (8), pressure drop was measured by total ten pressure taps as shown in Fig. 3 (a).

f_0 is calculated by Eq. (9) [7].

$$f_0 = \left[0.79 \ln(\mathrm{Re}_{D_h}) - 1.64\right]^{-2} \tag{9}$$

for $3000 < \mathrm{Re}_{D_h} < 5 \times 10^6$.

Table 1. Uncertainties in heat transfer measurement.

Variables	Typical value	Uncertainty
T_w	35.42℃	±0.2℃
T_m	27.75 - 41.2℃	±0.2℃
T_i	27.5℃	±0.2℃
$\sqrt{\alpha} / k_w$	0.0018634	5%
t	30sec	0.1sec
k_m	0.0263 W/mK	5%
Duct size	30mm×225mm	0.5mm
h	264.59 W/m^2K	12.9%
Nu	532.62	13.92%

The average and local Nusselt number is defined as Eq. (10) and $Nu_{D_h,0}$ can be calculated by Eq. (11) [7].

$$\overline{Nu_{D_h}} = \frac{\overline{h} D_h}{k_m} \tag{10}$$

$$Nu_{D_h,0} = \frac{(f_0/8)(\mathrm{Re}_{D_h} - 1000)\mathrm{Pr}}{[1 + 12.7(f_0/8)^{1/2}(\mathrm{Pr}^{2/3} - 1)]} \tag{11}$$

for $0.5 < \mathrm{Pr} < 2000$, $3000 < \mathrm{Re}_{D_h} < 5 \times 10^6$.

Since the transient liquid crystals technique is based on the one-dimensional assumption, test duration time should be limited so that the opposite side of test section can remain at the initial temperature. Wagner et al. [8] suggested criterion for the test duration time as Eq. (12).

$$\frac{\alpha t_{test\ duration}}{thickness^2} < \frac{1}{4} \tag{12}$$

For current test section, $t_{test\ duration}$ is about 180 seconds and the test duration time was kept less than 60 seconds.

Uncertainty in the measurement estimated numerically since Eq. (7) can not be expressed in explicit form regarding the heat transfer coefficient [9]. Table 1 shows uncertainties of each variable and resulting uncertainties of heat transfer coefficient and Nusselts number for typical test.

4. Result and discussion

Five different blockage walls with circular 7,9,11, narrow, and wide holes were used and tests were conducted at Re_{D_h} of about 20000, 30000, and 40000.

Fig. 5 presents the distribution of Nusselt number

for circular 9 holes case. Results clearly show the effect of jets. As the jet impinges on the downstream blockage walls, Nusselt number increases and Nusselt number between jets is relatively lower. The overall Nusselt number is higher for the second measurement plane. That is caused by increased mixing of mainstream flow. As the mainstream flow impinges repeatedly on the blockage wall, flow becomes more turbulent and the turbulence intensity on the second measurement plane becomes higher than that on the first measurement plane. The increased turbulence intensity on the second measurement plane results in higher heat transfer coefficient. Fig. 5 also shows that the overall Nusselt number increases as the Reynolds number increases.

Fig. 6 shows the distribution of Nusselt number for the narrow holes case. Compared to the circular 9 holes case (Fig. 5), the overall Nusselt number decreased due to narrower jet flow. The narrower jet could induce relatively less spanwise mixing and result in lower heat transfer. As Reynolds number increases, the overall Nusselt number also increases.

For the wide holes case (Fig. 7), high Nusselt number region by jet impingement is wider than circular or narrow holes cases. Compared to narrow holes case (Fig. 6), the overall Nusselt number is higher and the distribution of the Nusselt number becomes more uniform. Wider jet flow could induce more spanwise mixing and that would result in higher overall heat transfer coefficient on the measurement plane.

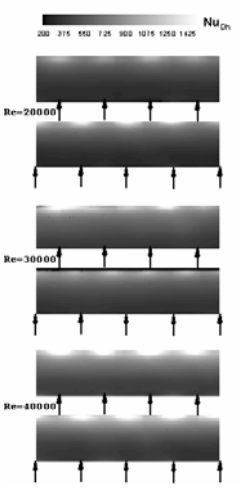

Fig. 5. Nusslet number distribution (circular 9holes).

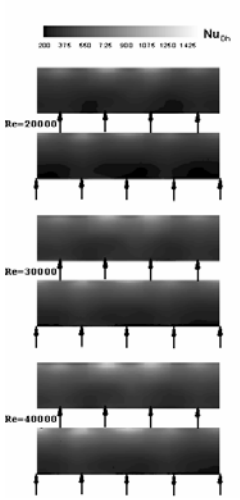

Fig. 6. Nusslet number distribution (narrow holes).

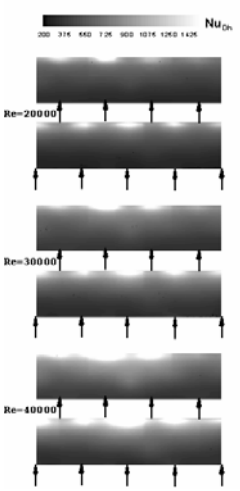

Fig. 7. Nusslet number distribution (wide holes).

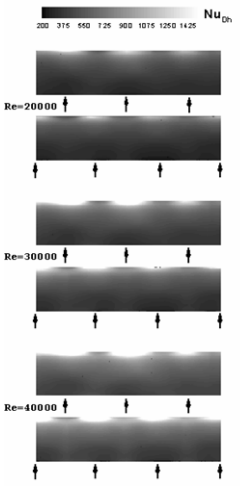

Fig. 8. Nusslet number distribution (circular 7 holes).

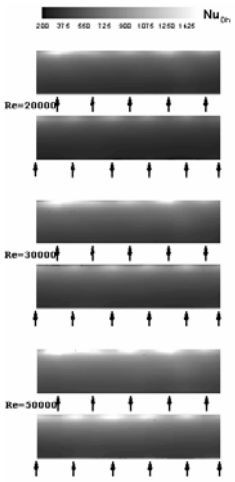

Fig. 9. Nusslet number distribution (circular 11 holes).

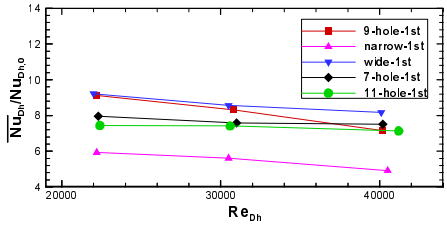

(a) Second plane

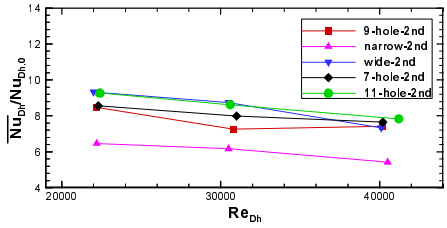

(b) Second plane

Fig. 10. Averaged Nusselt number.

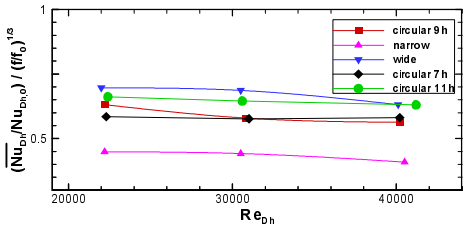

Fig. 11. Overall thermal performance factor.

Fig. 8 presents the distribution of Nusselt number for circular 7 holes case. Because the distance be tween holes is wider, the effect by jets can be easily recognized. In the circular 11 holes case (Fig. 9), due to the narrower hole distance, the distribution of the Nusselt number becomes more uniform.

Fig. 10 presents averaged Nusselt numbers on the first and second measurement planes. The averaged Nusselt numbers were normalized by the Nusselt number for smooth duct case (Eq. (11)) with same Reynolds number. For all cases, the averaged Nusselt number generally decreases as Reynolds number increases. For all Reynolds number, the averaged Nusselts number for the wide holes is highest and for the circular hole cases, 11 holes case is higher than 7 or 9 holes cases.

Fig. 11 shows the overall thermal performance factor for each case. The overall thermal performance factor was calculated using overall pressure drop across measurement planes and the averaged Nusselt number for both measurement planes. Generally, the overall performance factor decreases as Reynolds number increases, however, the variation of the thermal performance with Reynolds number was small. The wide hole case shows best thermal performance factor and as the number of hole increases for the circular hole cases, the thermal performance factor also increases

5. Conclusions

In this paper, improved hue detection based transient liquid crystal technique was used to measure heat transfer coefficient in a rectangular duct with blockage walls. Three different shapes of hole of wide, narrow, and circular holes were tested and for the circular hole cases, 7, 9, and 11 holes were tested. Reynolds number based on the duct hydraulic diameter was ranged from about 20000 to 50000. Result showed that the Nusselt number ratio and the overall thermal performance factor decreased as Reynolds number increased. For all Reynolds numbers tested, the wide holes case showed best performance. For the circular hole cases, the thermal performance factor was slightly increased as the number of hole was increased. The overall thermal performance factors for all cases were less than 1, however, results showed that the shape of hole could improve the thermal performance by blockage walls with holes. Future works are recommended to optimize the shape and configuration of the blockage walls.

Acknowledgments

This work was supported by the KARI under KHP

Dual-Use Component Development Program funded by the MKE and the Korea Research Foundation Grant funded by the Korean Government (MOEHRD, Basic Research Promotion Fund) (KRF-2006-331-D00073).

Nomenclature

C_d	:	Discharge coefficient of Venturi flow meter
c_p	:	Specific heat of test section ($J/kg\,K$)
d	:	Pipe diameter (m)
f	:	Friction factor
h	:	Heat transfer coefficient (W/m^2K)
k	:	Thermal conductivity ($W/m\,K$)
Nu	:	Nusselt number
$\overline{Nu}$	:	Averaged Nusselt number
Pr	:	Prandtl number
p	:	Pressure (Pa)
Q	:	Volume flow rate ($m^3/\sec$)
Re	:	Reynolds number
T	:	Temperature (℃)
t	:	Hue change time (sec)

Subscripts

D_h	:	Hydraulic diameter (m)
i	:	Initial state
j	:	Time step
m	:	Mainstream
w	:	Wall
0	:	Smooth duct

Greeks

α	:	Thermal diffusivity of test section (m^2/s)
β	:	Diameter ratio
ε	:	Coefficient of expansion
ρ	:	Density (kg/m^3)
Δ	:	Difference
τ	:	Time step change in Duhamel's theorem (sec)

References

S. V. Ekkad, G. Pamula and S. Acharya, 2000, Influence of crossflow-induced swirl and impingement on heat transfer in an internal coolant passage of a turbine airfoil, *J of heat transfer*, 122 587-597.

G. Pamula, S. V. Ekkad and S. Acharya, 2000, Influence of cross-flow induced swirl and impingement on heat transfer in a two-pass channel connected by two rows of holes, ASME paper 2000-GT-0235

S. W. Moon and S. C. Lau, 2003, Heat transfer between blockages with holes in a rectangular channel, *J. of heat transfer*, 125 587-594.

S. C. Lau, J. Cervantes, J. C. Han, R. J. Rudolph and K. Flannery, 2003, Measurements of wall heat (mass) transfer for flow through blockages with round and square holes in a wide rectangular channel, *Int. J. of heat and mass transfer*, 46 3991-4001.

S. Shin and J. S. Kwak, 2007, Improvement of the hue detection based transient liquid crystals technique, AICFM 2007-027, Jeju, Korea.

ISO, 2004, Measurement of fluid flow by means of pressure differential devices inserted in circular cross-section conduits running full-Part 4: Venturi tubes, ISO 5167-4.

F. P. Incropera and D. P. DeWitt, 2001, Heat and mass transfer, 5th edition, John Wiley & Sons, INC.

S. Wagner, M. Kotulla, P. Ott, B. Weigand, and V. von Wolfersdorf, 2005, The transient liquid crystal technique: Influence of surface curvature and finite wall thickness, *J. of Turbomacinery*, 127 175-182.

P. F. Dunn, 2005, Measurement and data analysis for engineering and science, Mcgraw-Hill, Inc.